Contribution from the School of Chemistry, University of New South Wales, P.O. Box 1, Kensington, NSW 2033, Australia

Aggregated Structures of the Compounds $Cd(SC_6H_4X\text{-}4)_2$ in DMF Solution

Ian G. Dance,* Robert G. Garbutt, and Trevor D. Bailey†

Received June 19, 1989

Substituted arenethiolate complexes $Cd(SC_6H_4X\text{-}4)_2$ (X = H (**1a**), F (**1b**), CH_3 (**1c**), Br (**1e**), Cl (**1e**)), which have been shown to be structurally nonmolecular in the solid state, require polar coordinating solvents such as DMF for dissolution. The ^{113}Cd NMR spectrum of **1a** at 224 K shows a major line at δ_{Cd} 593.1 ppm, diagnostic of cadmium surrounded by four thiolate ligands, and a minor (5%) line at 130 ppm ascribed to cadmium with $\{Cd(SPh)(DMF)_n\}^+$ coordination. With increasing temperature, only the major line is observed, broadening and then narrowing to a line at 458 ppm, at 341 K. Compounds **1b-e** give similar spectra. The temperature-dependent ^{13}C NMR spectra reveal the presence of rapidly interchanging bridging and terminal SAr ligands. The ^{113}Cd NMR spectral changes are interpreted in terms of the dynamics of interconversions between aggregated and deaggregated cadmium species. The preferred structural model for the aggregated species formed at low temperatures involves adamantanoid cages {*octahedro*-$(\mu\text{-}SAr)_6$-*tetrahedro*-Cd_4} linked through *vertices* by bridging thiolates, in the same manner as occurs in the various crystal structures. Ligand disproportionation equilibria such as $18Cd(SAr)_2(s) + DMF \rightarrow [Cd_{16}(SAr)_{34}(DMF)_2]^{2-} + [(DMF)_mCd(\mu\text{-}SAr)_2Cd(DMF)_m]^{2+}$ account for the coordinative dissolution, the low solution conductivity, and the high δ_{Cd} and low δ_{Cd} resonances. Various alternative vertex-linked polyadamantanoid aggregates of different sizes are postulated to exist in solution. To account for the changes in the ^{113}Cd NMR spectra, it is proposed that with temperature increase, smaller vertex-linked species with different sizes and degrees of solvent coordination are formed, in a cascade of increasingly rapid deaggregation reactions. An alternative structural model for the low-temperature aggregates, involving *fused* adamantanoid cages, is judged to be less plausible. Addition of small amounts of halide (Cl^-, Br^-, I^-) to solutions of $Cd(SAr)_2$ in DMF causes changes to the ^{113}Cd NMR spectra consistent with coordinated solvent being replaced by halide.

Introduction

The general insolubility of compounds of the type $Cd(SR)_2$ has curtailed access, via single-crystal diffraction, to information on their crystal structures. However, some compounds will dissolve in donor solvents such as DMF,[1] DMSO, and HMPA and in some cases crystallize unsolvated. Thus we have recently determined[2-4] the crystal structures of $Cd(SPh)_2$ (**1a**), $Cd(SC_6H_4F\text{-}4)_2$ (**1b**), $Cd(SC_6H_4CH_3\text{-}4)_2$ (**1c**), and $Cd_8(SC_6H_4Br\text{-}4)_{16}(DMF)_3$ (**1d**). Crystals of $Cd(SC_6H_4Cl\text{-}4)_2$ (**1e**), decomposed on X-irradiation, but it could be determined that the lattice of **1e** is different from those of the analogous compounds. We have also determined the crystal structure of $Cd(SC_6H_4CH_3\text{-}2)_2$ (**2**),[5] which is different from all of the aforementioned compounds. A characteristic of all of these crystalline compounds is structural nonmolecularity. Furthermore, in all except the 2-substituted benzenethiolate derivative **2**,[5] the crystals are composed of adamantanoid cage units linked by the sharing of vertices. The tetrahedral adamantanoid cage is characterized by an {*octahedro*-$(\mu\text{-}SAr)_6$-*tetrahedro*-Cd_4} core with four terminal SAr ligands, and in all four structures **1a-d**, the nonmolecularity is achieved by thiolate ligands functioning as intercage bridges. In **1a-c** all four terminal positions of each adamantanoid cage are bridged, in different three dimensionally nonmolecular patterns. The crystal structure of **1d** is two dimensionally nonmolecular, with each adamantanoid cage linked to three neighbors by bridging thiolates: half of the cages have terminal thiolate at the fourth Cd atom, while the remainder of the cages have three DMF ligands coordinated to the fourth Cd atom. A single adamantanoid cage $[(\mu\text{-}SPh)_6Cd_4(SPh)_4]^{2-}$ occurs in the molecular structure of $[Cd_4(SPh)_{10}]^{2-}$ (**3**, Me_4N^+ salt), which together with numerous heteroligated derivatives have been well-characterized in crystals and in solution.[6-9] The adamantanoid cage structure is paradigmatic for molecular metal thiolate compounds.[10]

On dissolution of these nonmolecular $Cd(SAr)_2$ compounds in DMF, some degree of bridge breaking must occur, creating species (charged or uncharged) that are structurally molecular. The sizes and structures of the dissolved species are of considerable interest, particularly as the recrystallization incorporates little or no coordinated solvent. Previous investigations of the behavior of a variety of molecular cadmium thiolate complexes in solution have made considerable use of ^{113}Cd NMR ($I = {}^1/_2$) at natural abundance (12.26%),[8,9,11-17] and it is against this background of correlated solid-state structures and solution ^{113}Cd NMR data that we have investigated solutions of $Cd(SAr)_2$ by ^{113}Cd and ^{13}C NMR in order to obtain information about the molecular species and their structures in solution. In our first communication[2] we suggested that the molecule $[Cd_{10}(SPh)_{20}]$ (**4**) (for which there is structural precedent in related systems) could occur in these solutions. We now believe this to be unlikely and examine other interpretations.

Results and Discussion

Conductivity. Conductivity measurements were obtained for DMF solutions of $Cd(SPh)_2$ (**1a**) at a range of concentrations. For comparison, measurements were obtained under similar conditions for the 1:1 electrolyte Bu_4NI, and the 2:1 electrolyte $(Me_4N)_2[Cd_4(SPh)_{10}]$ (**3**). No anomalies were observed in the concentration dependence of the conductivities, and comparisons were made for 10^{-3} M solutions. Values of Λ_M at this concentration were 5 S cm^2 mol^{-1} for $Cd(SPh)_2$ (**1a**), 72 S cm^2 mol^{-1} for Bu_4NI, and 106 S cm^2 mol^{-1} for $(Me_4N)_2[Cd_4(SPh)_{10}]$. The value for Bu_4NI is within the range expected[18] for a 1:1 electrolyte in DMF, while that for $(Me_4N)_2[Cd_4(SPh)_{10}]$ is somewhat low for a 2:1 electrolyte. However, the extremely low value obtained for the $Cd(SPh)_2$ solution indicates that the species formed when

† Present address: School of Business and Technology, Macarthur Institute of Higher Education, P.O. Box 555, Cambelltown, NSW 2560, Australia.

(1) The solubility of $Cd(SPh)_2$ in DMF has been noted previously: Barabash, Y. V.; Skrypnik, Y. G.; Shevchuk, I. A.; Korotkova, Z. G. *J. Anal. Chem. USSR (Engl. Transl.)* **1979**, *34*, 1163.
(2) Craig, D.; Dance, I. G.; Garbutt, R. *Angew. Chem., Int. Ed. Engl.* **1986**, *25*, 165.
(3) Dance, I. G.; Garbutt, R. G.; Craig, D. C.; Scudder, M. L.; Bailey, T. D. *J. Chem. Soc., Chem. Commun.* **1987**, 1164.
(4) Dance, I. G.; Garbutt, R. G.; Craig, D. C.; Scudder, M. L. *Inorg. Chem.* **1987**, *26*, 4057.
(5) In **2** the structure is composed of linked $M_3(\mu\text{-}SR)_3$ cycles and $M_2(\mu\text{-}SR)_2$ cycles: Dance, I. G.; Garbutt, R. G.; Scudder, M. L. *Inorg. Chem.*, in press.
(6) Hagen, K. S.; Stephan, D. W.; Holm, R. H. *Inorg. Chem.* **1982**, *21*, 3928.
(7) Hagen, K. S.; Holm, R. H. *Inorg. Chem.* **1983**, *22*, 3171.
(8) Dean, P. A. W.; Vittal, J. J. *Inorg. Chem.* **1986**, *25*, 514.
(9) Dean, P. A. W.; Vittal, J. J.; Payne, N. C. *Inorg. Chem.* **1987**, *26*, 1683.
(10) Dance, I. G. *Polyhedron* **1986**, *5*, 1037.
(11) Dean, P. A. W.; Vittal, J. J. *J. Am. Chem. Soc.* **1984**, *106*, 6436.
(12) Dean, P. A. W.; Vittal, J. J. *Inorg. Chem.* **1985**, *24*, 3722.
(13) Dance, I. G.; Saunders, J. K. *Inorg. Chim. Acta* **1985**, *96*, L71.
(14) Dance, I. G. *Inorg. Chim. Acta* **1985**, *108*, 227.
(15) Dance, I. G. *Aust. J. Chem.* **1985**, *38*, 1745.
(16) Dance, I. G.; Garbutt, R.; Craig, D. C. *Aust. J. Chem.* **1986**, *39*, 1449.
(17) Summers, M. F. *Coord. Chem. Rev.* **1988**, *86*, 43.
(18) Geary, W. J. *Coord. Chem. Rev.* **1971**, *7*, 81.

0020-1669/90/1329-0603$02.50/0

Table I. ^{113}Cd NMR Chemical Shifts (ppm)[a] of $Cd(SAr)_2$ Species

compd	at 224 K: ≥95% intensity	at 224 K: ≤5% intensity	>300 K
$Cd(SPh)_2$ (**1a**)	593	130	458 (341 K)
$Cd(SC_6H_4F\text{-}4)_2$ (**1b**)	597	128	441 (330 K)
$Cd(SC_6H_4CH_3\text{-}4)_2$ (**1c**)	593	130	472 (330 K)
$Cd(SC_6H_4Br\text{-}4)_2$ (**1d**)	595	126	
$Cd(SC_6H_4Cl\text{-}4)_2$ (**1e**)	596	128	

[a] Relative to 0.1 M aqueous $Cd(NO_3)_2$, which resonates at −3.9 ppm relative to 0.1 M aqueous $Cd(ClO_4)_2$ and -5 ppm relative to $Cd(ClO_4)_2$ at infinite dilution.

$Cd(SPh)_2$ dissolves in DMF have a very low charge to size ratio. In view of the pronounced activation of small anions such as PhS^- as nucleophiles in aprotic solvents, ligand dissociation (such as eq 3) is less probable than ligand disproportionation, according

$$6Cd(SPh)_2(s) \rightarrow [Cd_4(SPh)_{10}]^{2-} + 2[Cd(SPh)(DMF)_m]^+ \quad (1)$$

$$6Cd(SPh)_2(s) \rightarrow [Cd_4(SPh)_{10}]^{2-} + [(DMF)_mCd(\mu\text{-}SPh)_2Cd(DMF)_m]^{2+} \quad (2)$$

$$4Cd(SPh)_2(s) \rightarrow [Cd_4(SPh)_7(DMF)_m]^+ + PhS^- \quad (3)$$

to equations such as (1) or (2), as the mechanism for generation of charged species. The observed conductivity indicates that 20–30% of the $Cd(SPh)_2$ could dissolve according to reactions 1 or 2. However, larger anionic species can be envisaged, and for example, the observed conductivity would be consistent with more than 50% of dissolution according to eqs 4 or 5.

$$18Cd(SPh)_2(s) \rightarrow [Cd_{16}(SPh)_{34}]^{2-} + 2[Cd(SPh)(DMF)_m]^+ \quad (4)$$

$$18Cd(SPh)_2(s) \rightarrow [Cd_{16}(SPh)_{34}]^{2-} + [(DMF)_mCd(\mu\text{-}SPh)_2Cd(DMF)_m]^{2+} \quad (5)$$

^{113}Cd NMR Spectra. At low temperature, 224 K, the ^{113}Cd NMR spectrum of **1a** in DMF (see Figure 1) contains one major line with 95% of the total intensity at 593.1 ppm (half-width 137 Hz), and a minor line with the remaining 5 (±1)% intensity at 130 ppm.[19] As the temperature is raised, the major line broadens and then resharpens: at the highest temperature of measurement, 341 K,[20] the chemical shift is 458 ppm and the half-width 480 Hz. The minor line at 130 ppm is not detectable (presumably due to broadening) at temperatures above 224 K. Very similar spectra and changes with temperature are observed for other related $Cd(SAr)_2$ compounds, and the positions of the lines observed at 224 K and at temperatures above 300 K are reported in Table I.

The Cd resonance at 593 ppm in the 224 K spectrum of $Cd(SPh)_2$ is diagnostic of Cd coordinated by four SPh ligands, a $\{Cd(SPh)_4\}$ coordination site,[21] and therefore requires a species with thiolate bridging. It is significant that the single resonance of **3**, for the $\{(\mu\text{-}SPh)_3CdSPh\}$ site, occurs at 594.0 ppm when measured under the same temperature and solvent conditions. Since at 224 K the spectrum of $Cd(SPh)_2$ has not fully attained the slow-exchange limit, it is not possible to assert any difference between the low-temperature Cd spectra of **1a** and of **3** in this region.

The minor resonance at ca. 130 ppm, observable only at low temperature, occurs in a chemical shift region not previously entered by cadmium thiolate species, which appears to indicate a solvated complex with only one SPh ligand in the coordination sphere of each cadmium atom, i.e. $\{Cd(SPh)(DMF)_m\}$. The shift of this resonance responds very slightly to variation of the thiolate

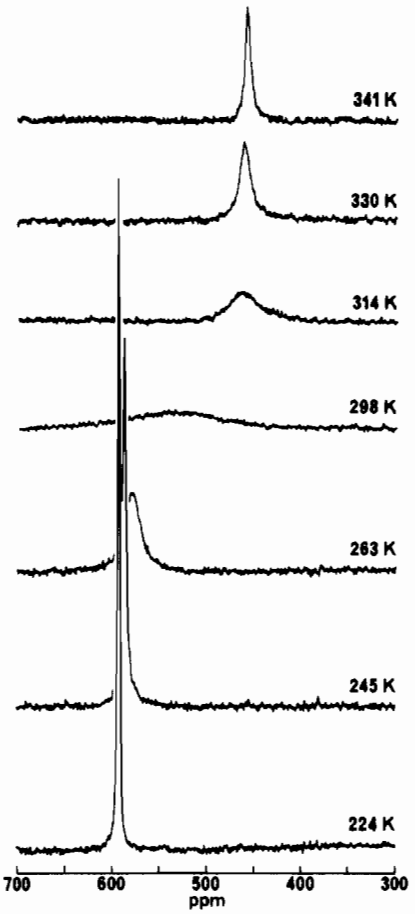

Figure 1. ^{113}Cd NMR spectra (66.6 MHz, natural abundance ^{113}Cd) of $Cd(SPh)_2$ (**1a**) in DMF (ca. 1 g/3 mL) at the temperatures marked. A very weak line at 130 ppm, observed only at the lowest temperature, is not shown.

substituent. Our interpretation of the 130 ppm resonance is that it is due to species such as $[Cd(SPh)(DMF)_m]^+$ (or $[(DMF)_mCd(\mu\text{-}SPh)_2Cd(DMF)_m]^{2+}$) generated by ligand disproportionation reactions such as (1), (2), (4), or (5). The resonances of the $\{Cd(SPh)_4\}$ sites in the other products of these reactions are accounted for by the 593 ppm resonance at low temperature. The nonobservation of the 130 ppm resonance at all temperatures except the lowest is consistent with the rapid ligand exchange rate expected for $[Cd(SPh)(DMF)_m]^+$, and is supported by the ^{13}C NMR data (see below).

The 458 ppm limiting resonance of **1a** at high temperature is consistent with $\{Cd(SPh)_3(DMF)_m\}$ coordination,[22] again requiring species with some thiolate bridging. Cadmium with this coordination has not previously been characterized *in solution*, but its chemical shift can be estimated as 434 ppm by linear proportion between the $\{Cd(SAr)_4\}$ site at 590 ppm and $[Cd(DMF)_n]^{2+}$, which we have measured as −35 ppm at 220 K for $Cd(BF_4)_2$ in DMF. An alternative estimate, using the "pairwise additivity model"[23,24] in an attempt to take into account the nonlinearity known in related systems[25] and using the assumption that the minor line at 130 ppm is due to $\{Cd(SPh)(DMF)_m\}$, yields the similar value of 442 ppm for the chemical shift of a $\{Cd(SAr)_3(DMF)_m\}$ site. In some of the low-temperature spectra that we have measured, there is evidence of a very broad but weak resonance absorption in the vicinity of 350 ppm: this could be due to a severely broadened $\{Cd(SAr)_2(DMF)_m\}$ average site.

(19) The intensity of the minor line does not diminish with repeated sample purification.
(20) The studies reported in the communication[2] did not extend to the upper temperature range and the fast-exchange spectra.
(21) Braces { } define a Cd coordination environment.
(22) The number *m* of coordinated DMF ligands is not specified in most formulas in this paper. There is precedent for both $[Cd(\mu\text{-}SAr)_3(DMF)_3]^3$ and $[Cd(\mu\text{-}SAr)_4(DMF)]$ in crystals, but with long Cd–DMF bonds in the latter.[5]
(23) Vladimiroff, T.; Malinowski, E. R. *J. Chem. Phys.* **1967**, *46*, 1830.
(24) Kidd, R. G.; Spinney, H. G. *Inorg. Chem.* **1973**, *12*, 1967.
(25) Colton, R.; Dakternieks, D. *Aust. J. Chem.* **1980**, *33*, 2405.

Table II. ^{13}C Chemical Shifts (ppm) for Terminal (t) and Bridging (br) Ligands in **1a** and **3** at 223 K.

	C_1 t/br	C_2, C_6 br/t	C_3, C_5 br/t	C_4 t/br
1a	145.0/136.9	134.8	129.4	125.8/123.4
3	145.6/137.1	134.7/134.0	129.2/129.0	125.5/122.7

In general terms, the spectral features shown in Figure 1 are consistent with the occurrence of aggregated complexes with thiolate bridges and $\{Cd(SPh)_4\}$ sites at low temperature and, at high temperatures, the occurrence of *partially* deaggregated species with additional $\{Cd(SAr)_n(DMF)_m\}$ sites ($n = 2, 3$), which are in fast exchange. Considering first the general dynamics of the system and deferring speculation about the possible structures of the aggregates, we use equations of type (6) to refer to each of several possible stages in the deaggregation/aggregation equilibria.

$$\text{larger aggregates} + \text{DMF} \underset{k_{agg}}{\overset{k_{deagg}}{\rightleftharpoons}} \text{smaller aggregates} \quad (6)$$

The rate k_{deagg} must increase with temperature more rapidly than k_{agg}, such that at low temperature, $k_{deagg} \ll k_{agg}$, and only the most aggregated species are present in detectable concentrations. At high temperature there are appreciable concentrations of deaggregated species, but in this temperature regime, there is NMR fast exchange of Cd sites. At temperatures where k_{deagg} is sufficiently larger than k_{agg} to allow detectable concentrations of deaggregated species at lower chemical shifts, it is large enough to cause exchange broadening. Alternatively stated, when the temperature is reduced, all sites contributing to the exchange average are not revealed because the equilibrium of the species containing them is shifted almost fully in favor of aggregates containing only one type of site. Even though it is not possible to observe the chemical shifts of all exchange-averaged sites, it can be estimated that $\Delta\nu$ for them is at least 140 ppm or 10^4 Hz and thus that k_{agg} and k_{deagg} are on the order of 10^4 s^{-1} at ca. 300 K.

The implication of this interpretation of the temperature dependence is that $\Delta H^*_{deagg} > \Delta H^*_{agg}$, which is entirely reasonable and consistent with the expectation that $\Delta S^*_{deagg} > \Delta S^*_{agg}$. As the aggregates become smaller there is a cascade of deaggregation and decreasing ΔH^*_{deagg}.

^{13}C NMR Spectra. The ^{13}C NMR spectra of **1a** at temperatures varying from 223 to 298 K are shown in Figure 2. At 298 K there is one set of four ligand resonances, averaged by exchange, but at the lower temperatures there is broadening and (at 223 K) splitting of the C_1 and C_4 resonances, corresponding to the bridging and terminal SPh ligands. These spectra are similar to (but different from) those for **3**: the comparable chemical shifts at 223 K are contained in Table II. From the ^{13}C spectra the rate of bridging $\rightleftharpoons$ terminal ligand interchange in **3** is estimated to be about 4×10^4 s^{-1} at 298 K. Bridging $\rightleftharpoons$ terminal ligand exchange was first described for $[M_4(SPh)_{10}]^{2-}$ (M = Fe, Co, Zn, Cd) from ^1H NMR data:[6] the mechanism proposed[6] for **3** is feasible for the linked adamantanoid cage structures postulated below. ^{13}C NMR spectra of other $Cd(SAr)_2$ compounds in DMF are similar to those of **1a**: although these spectra still show exchange broadening at the lowest temperatures, it appears that, at least at low temperatures, the species in solutions of $Cd(SAr)_2$ in DMF contain bridging and terminal SAr ligands similar to those of the adamantanoid cage $[Cd_4(SPh)_{10}]^{2-}$.

Possible Aggregate Structures. It is clear that most of the species in these solutions contain sites with $\{Cd(SAr)_4\}$ and $\{Cd(SAr)_3(DMF)_m\}$ (or average $\{Cd(SAr)_3(DMF)_m\}$) coordination and therefore must be aggregates with appreciable numbers of SAr bridges. We focus first on possible structures for the larger aggregates that predominate at low temperature, in which it appears that all Cd sites have $\{Cd(SAr)_4\}$ coordination. There are two structure types to present and discuss: first a molecular structure with *fused* adamantanoid cages and no coordinated DMF and then a series of *vertex-linked* adamantanoid cages and varying proportions of peripheral coordination by DMF.

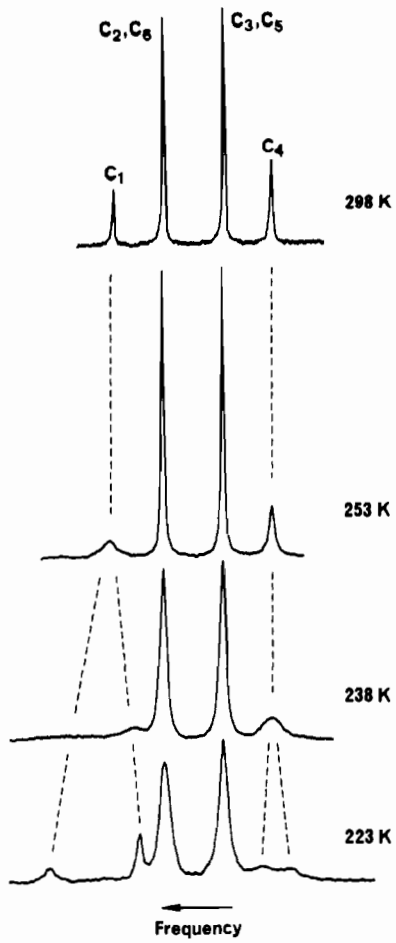

Figure 2. Proton-decoupled ^{13}C NMR spectra of $Cd(SPh)_2$ (**1a**) in DMF solution at the temperatures marked. The slow-exchange regime for bridging (br) and terminal (t) SPh ligands is not fully attainable experimentally. The spectra have been displaced horizontally to compensate for the temperature dependence of δ_C. At the lowest temperature the δ_C values relative to TMS are as follows: $^tC_1$, 145.0; $^{br}C_1$, 136.9; C_2, C_6, 134.8; C_3, C_5, 129.4; $^{br}C_4$, 125.8; $^tC_4$, 123.4.

The smallest *molecular* structure that can be proposed to yield $\{Cd(SAr)_4\}$ coordination only, within the constraint of the 2:1 PhS:Cd stoichiometric ratio, is the tetra-fused adamantanoid aggregate $Cd_{10}(SAr)_{20}$ (**4**), i.e. *tetrahedro*-$(\mu_3\text{-}SAr)_4$-*octahedro*-

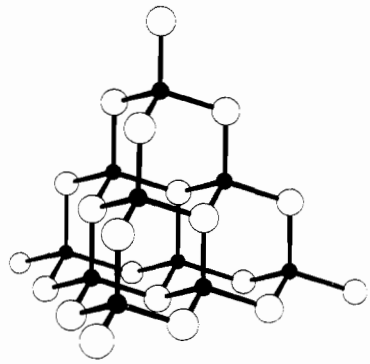

4

Cd_6-*truncated-tetrahedro*-$(\mu\text{-}SAr)_{12}$-*tetrahedro*-$(CdSAr)_4$. This is a derivative of the known aggregate $[(\mu_3\text{-}S)_4Cd_{10}(\mu\text{-}SPh)_{12}(SPh)_4]^{4-}$ (**5**),[26] but with μ_3-SAr in place of μ_3-S. Prior stereochemical analysis[26] for **5** has established the absence of steric interference between phenyl substituents in **4**. The confirmed crystal structures of the fused tetraadamantanoid aggregates

(26) Dance, I. G.; Choy, A.; Scudder, M. L. *J. Am. Chem. Soc.* **1984**, *106*, 6285.

Table III. Possible Species in $Cd(SAr)_2$/DMF Solutions

structure	formula	av $\{Cd(SAr)_x\}$ coord	terminal (SAr)/ bridging (SAr) ratio
4	$Cd_{10}(SAr)_{20}$	$\{Cd(SAr)_4\}$	*a*
8	$Cd_{16}(SAr)_{32}(DMF)_4$	$\{Cd(SAr)_{3.75}(DMF)_{0.25}\}$	1/7
9	$Cd_{36}(SAr)_{72}(DMF)_6$	$\{Cd(SAr)_{3.833}(DMF)_{0.167}\}$	1/11
10	$Cd_{24}(SAr)_{48}(DMF)_6$	$\{Cd(SAr)_{3.75}(DMF)_{0.25}\}$	1/7
11	$Cd_{16}(SAr)_{32}(DMF)_2$	$\{Cd(SAr)_{3.875}(DMF)_{0.125}\}$	1/15
12	$[Cd_{16}(SAr)_{34}(DMF)_2]^{2-}$	$\{Cd(SAr)_{3.875}(DMF)_{0.125}\}$	3/14
13	$[Cd_{16}(SAr)_{34}]^{2-}$	$\{Cd(SAr)_4\}$	2/15
14	$Cd_4(SAr)_8(DMF)_2$	$\{Cd(SAr)_{3.5}(DMF)_{0.5}\}$	1/3
15	$Cd_2(SAr)_6(DMF)_2$	$\{Cd(SAr)_3(DMF)\}$	1/1

[a] There are two types of bridging SAr ligand: the ligand distribution is $(\mu_3\text{-}SAr)_4(\mu\text{-}SAr)_{12}(SAr)_4$.

$[Cd_{10}(SCH_2CH_2OH)_{16}]^{4+}$ (**6**)[27,28] and $[Cd_{10}(SCH_2CH_2OH)_{16}Cl_4]$ (**7**)[16] with μ_3-SCH_2CH_2OH ligands (chelating) support the plausibility of **4**. There are two slightly different $\{Cd(SAr)_4\}$ sites in **4**, namely $\{(\mu_3\text{-}SAr)_2(\mu\text{-}SAr)_2Cd^i\}$ and $\{(\mu\text{-}SAr)_3Cd^oSAr\}$ (i and o signify inner and outer, respectively), and the above interpretation requires that their resonances be separated by not more than 2 ppm within the 493 ppm envelope: this is in general accord with the body of Cd NMR data on cadmium thiolates, but detailed data that would allow account of the subtle differences in charge distribution between these sites are not available. The fused polyadamantanoid structure of $Cd_{10}(SAr)_{20}$ would be expected to be rigid, like that of **5** and thus like **5** display ^{113}Cd–$^{111,113}Cd$ coupling,[13,15] but the magnitude of the coupling would be ca. 40 Hz and not resolved in the broader resonances of the $Cd(SAr)_2$/DMF solutions.

There are three difficulties with the postulate of **4** as the aggregate predominating at low temperature. One is that the $Cd(SAr)_2$ compounds dissolve only in the donor solvents such as DMF, HMPA, and DMSO, implying that some coordination by these solvents is involved in the solution species. The uncharged molecule **4** could be expected to exist in other less coordinating solvents. The other difficulty is that **4** is composed of *fused* adamantanoid cages, unlike the vertex-linked adamantanoid cages in crystalline **1a–d**, and therefore aggregation and deaggregation reactions involving **4** (as well as the crystallization and dissolution of **1**) would incur large degrees of cage rearrangement and concerted bond disruptions. It is difficult to conceive of mechanisms accounting for the observed rapid rates of aggregation and deaggregation. It is known[15] that the exchange reactions in DMF of the fused tetraadamantanoid cage species $[E_4M_{10}(SPh)_{16}]^{4-}$ (E = S, Se; M = Zn, Cd) occur on the time scale of hours for the inner metal atoms M^i. Processes that interconvert fused adamantanoid cages and vertex-linked adamantanoid cages are expected to meet mechanistic barriers similar to those for exchange of the core atoms of fused cages and therefore to be very much slower than the observed exchange rates. The third difficulty is that three types of SAr ligands occur in **4**, whereas only two have been resolved in the ^{13}C NMR spectrum.

The alternative and preferred postulate for the structures of species present in DMF solutions of $Cd(SAr)_2$ at low temperatures involves oligomers of vertex-linked adamantanoid cages, with structures analogous to molecular fragments of crystalline **1a–d**. The general formulation of these postulated structures is $[Cd_4(SAr)_8]_p$, but in order to maintain 4-fold coordination of cadmium, a small proportion of additional peripheral ligands would be required only at one cadmium site in some of the peripheral cages: when the additional ligands are DMF, the general formulation of the oligomer is $[Cd_4(SAr)_8]_p(DMF)_q$. These structures contain (μ-SAr) ligands that are within the adamantanoid cages and that link the adamantanoid cages. The numerous one-, two-, and three-dimensional connectivity patterns possible and known for tetrahedra linked through vertices would be available to these oligomers of condensed adamantanoid cages. Figure 3 illustrates four possible vertex-linked adamantanoid oligomers, **8–11**, and identifies positions for terminally coordinated heteroligands.

One type, the condensed two-dimensional net, is exemplified by **8** and **9**. With, in general, $a \times b$ adamantanoid cages, this type would have the composition $[Cd_4(SPh)_8]_{ab}(DMF)_{a+b}$, with $6ab$ intracage (μ-SPh) ligands, $(2ab - a - b)$ intercage (μ-SPh) ligands, and an average coordination $\{Cd(SPh)_{4-x}(DMF)_x\}$, where $x = (a + b)/4ab$ and $(8ab - a - b)/(a + b)$ is the ratio of bridging to terminal SPh ligands. When $a = b = 2$ (**8**), $x = 0.25$; when $a = b = 4$, $x = 0.125$.

Cyclic two-dimensional nets of vertex-linked adamantanoid cages are also possible, the simplest being **10**, with average coordination $\{Cd(SPh)_{3.75}(DMF)_m\}$ and a bridging to terminal thiolate ratio of 7.

The simplest three-dimensional net is $[Cd_4(SPh)_8]_4(DMF)_2$ (**11**) with four cages at the vertices of a tetrahedron, average coordination $\{Cd(SPh)_{3.875}(DMF)_m\}$, and a bridging to terminal thiolate ratio of 15.

Clearly it is possible to postulate oligo-linked adamantanoid cage aggregates in which the influence of the heteroligand DMF on the average coordination $\{Cd(SAr)_{4-x}(DMF)_x\}$ diminishes below a level that can be differentiated by δ_{Cd} at the lowest temperature. However, in the uncharged $[Cd_4(SAr)_8]_p(DMF)_q$ aggregates exemplified by **8–11**, the requirement for larger polycadmium species to decrease x to satisfy the ^{113}Cd NMR spectrum results in a ratio of terminal SAr to bridging SAr ligands generally less than the approximate value of 3 obtained from the ^{13}C NMR spectrum of **1a** at 223 K.[29] The conductivity data and the presence of the 130 ppm line in the ^{113}Cd NMR spectra show that some disproportionation of SAr ligands occurs, which will decrease x and increase the ratio of terminal to bridging SAr ligands, reducing the discrepancy between the ^{113}Cd and ^{13}C NMR data. Species **12** and **13** (see Table III) represent the modifications of **8** and **11**, respectively, in which two DMF ligands are replaced by two terminal SAr ligands, consistent with eqs 4 and 5 and the NMR data.

The postulate of vertex-linked adamantanoid cages for the structures of the aggregates in solution also allows a straightforward account of the structural and kinetic aspects of the deaggregation processes that occur at temperatures above 224 K. Various deaggregated species with decreasing proportions $(4 - x)$ of SAr in the Cd coordination $\{Cd(SAr)_{4-x}(DMF)_m\}$ can be proposed to account for the decreasing average δ_{Cd} as temperature increases. The disubstituted monoadamantanoid cage $[Cd_4(SAr)_8(DMF)_2]$ has $(4 - x) = 3.5$, and dissociation of this adamantanoid cage leads to the edge-shared bitetrahedral molecule $[(DMF)(SAr)Cd(\mu\text{-}SAr)_2Cd(SAr)(DMF)]$ which has $(4 - x) = 3$. This type of structure has been reported for $[Cd_2(SPh)_6]^{2-}$.[30] Cyclic oligomers of vertex-linked coordination tetrahedra, $[(\mu\text{-}SAr)Cd(SAr)(DMF)]_p$, also have $(4 - x) = 3$. At the limit of deaggregation by DMF, $[Cd(SAr)_2(DMF)_2]$ has $(4 - x) = 2$.

As the size of the molecule decreases the rate of deaggregation would be expected to increase, consistent with the rapid onset of a fast-exchange regime with temperature increase above ca. 270 K. The cascade of increasingly rapid deaggregations as the deaggregation proceeds is readily accommodated by this general structural model.

There is support from crystal structures for the proposed solution species and structures. Crystalline **1d** contains vertex-linked adamantanoid cages with one-eighth of the Cd atoms coordinated terminally by three DMF molecules: the structural formula is $^2_\infty[((\mu\text{-}SAr)_{15}Cd_6)(CdSAr)(Cd(DMF)_3)].$[3,31] Zinc benzenethiolate crystallizes from solutions containing methanol as

(27) Strickler, P. *J. Chem. Soc. D* **1969**, 655.
(28) Lacelle, S.; Stevens, W. C.; Kurtz, D. M., Jr.; Richardson, J. W., Jr.; Jacobson, R. A. *Inorg. Chem.* **1984**, *23*, 930.
(29) The ^{13}C intensity data with residual exchange broadening are regarded as less reliable than the δ_{Cd} measurement as indicators of the size of the aggregate in DMF solutions of **1a** at low temperature.
(30) Abrahams, I. L.; Garner, C. D.; Clegg, W. *J. Chem. Soc., Dalton Trans.* **1987**, 1577.
(31) Dance, I. G.; Garbutt, R.; Craig, D. C.; Scudder, M. L. Manuscript in preparation.

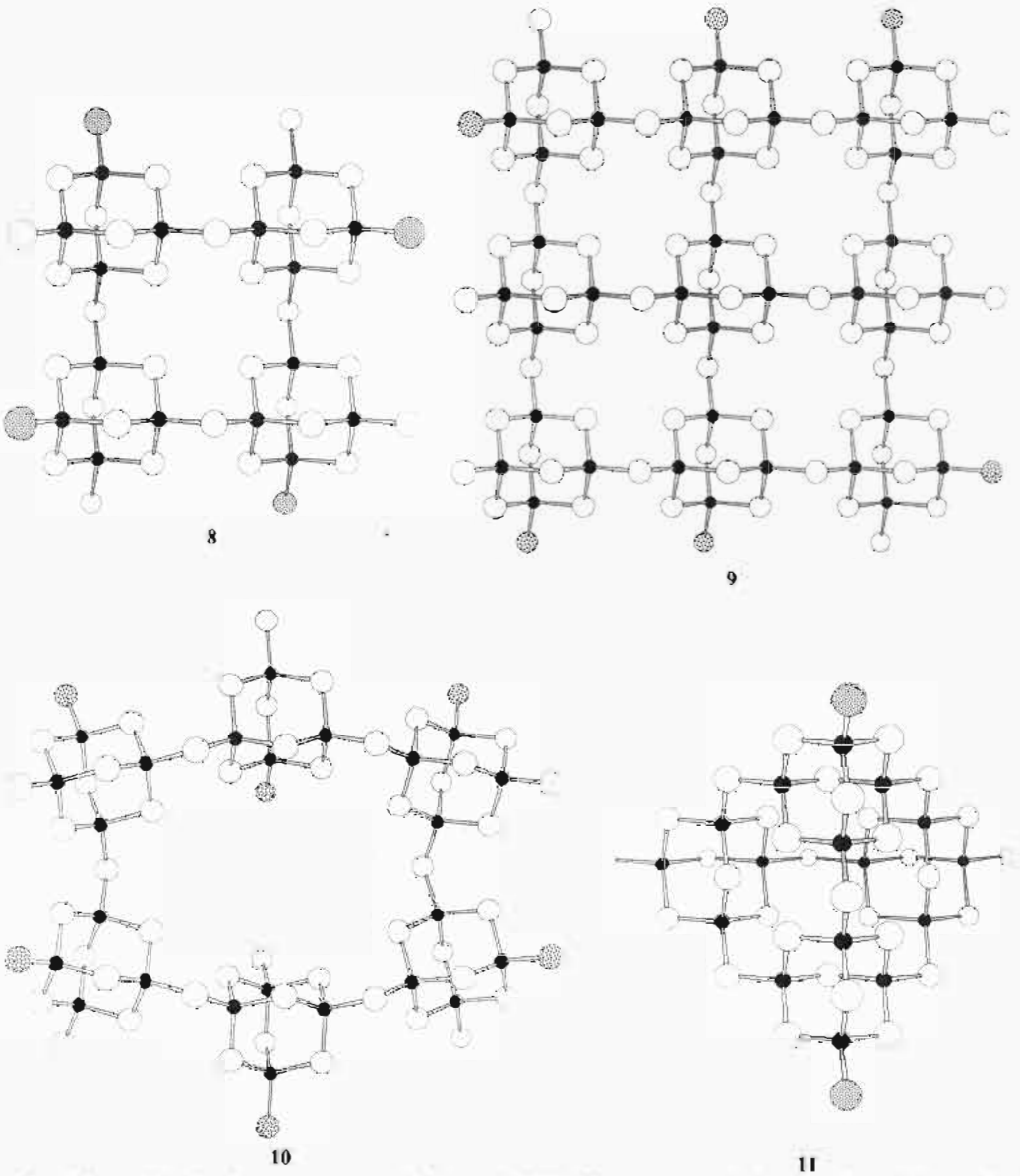

Figure 3. Frameworks of the possible oligo-linked adamantanoid molecules **8–11**. Cd atoms are marked as small dark circles, and the S atoms of SAr ligands are marked as larger white circles. All Ar groups are omitted, for clarity. The atoms marked as dotted circles are terminal DMF molecules in **8–11** but may also be terminal SAr ligands in the proposed anionic species such as **12** and **13**. These diagrams portray the connectivity, but not necessarily the three-dimensional conformation, of the models.

$^1_\infty[(\mu\text{-SPh})_6Zn_4(\mu\text{-SPh})(SPh)(CH_3OH)]$ in which each adamantanoid cage is thiolate bridged to others at two terminal positions and has an SPh ligand at one terminal position and coordinated methanol at the fourth.[32]

Effect of Halide Ions on $Cd(SAr)_2$ in Solution. The oligo-linked adamantanoid cage molecules postulated to occur in solution would be expected to be electrophilic at the terminal sites where solvent is coordinated, and this has been tested by addition of anionic ligands to the solutions. The addition of very small proportions of halide ion (X^-) to the $Cd(SPh)_2$/DMF solution has a pronounced effect on the Cd NMR spectra. An additional group of very closely spaced, relatively narrow (ca. 35 Hz), resonances appear (at 224 K) at 568 ppm for Cl^-, 552 ppm for Br^-, and 524 ppm for I^-. These resonances are due to $\{Cd(SPh)_3X\}$ coordination sites.[33] The intensity of the additional resonance increases in proportion to $Q = [X]/[Cd(SPh)_2]$ up to $Q \approx 0.3$, at which ratio it accounts for ca. 40% of the total Cd intensity. The most probable interpretation of these spectral changes involves the formation (virtually stoichiometric in X^-) of aggregated species involving sites of types $\{(\mu\text{-SPh})_3CdSPh\}$ and $\{(\mu\text{-SPh})_3CdX\}$, which are in slow exchange at 220 K. The resonances in each solution broaden with temperature increase, and the two resonance regions coalesce at about 300 K, due to exchange of terminal PhS^- and X^- ligands.

The splitting in both the $\{Cd(SPh)_4\}$ and $\{Cd(SPh)_3X\}$ regions is into three resonances of different intensity, separated by 0.5–1.0 ppm.[34] Such fine structure is very probably due to the presence of very similar species that differ only by X/SPh substitution three or more bonds distant in the adamantanoid cages. This interpretation is supported by data on shifts of δ_{Cd} due to transmitted electronic effects in the tetra-fused adamantanoid structure of $[E_4M_{10}(SPh)_{16}]^{4-}$ (**5**, M = Zn, Cd; E = S, Se), where the influence of E = S/Se substitution three bonds away is 1.5–3 ppm and the influence of M = Cd/Zn substitution four bonds distant is 3 ppm.[15]

(32) Dance, I. G. *J. Am. Chem. Soc.* **1980**, *102*, 3445.

(33) Our chemical shifts are consistent with those reported by Dean[12] for these coordination sites (X = Br, I; X ≠ Cl) in terminally substituted monoadamantanoid cages $[(\mu\text{-SPh})_6(CdSPh)_{4-y}(CdX)_y]^{2-}$ in acetone at 295 K.

(34) Dean[12] has commented that the broader lines observed at room temperature for $[Cd_4(SPh)_{10-x}X_x]^{2-}$ species were asymmetric, indicative of this splitting.

It is also possible that the solutions with the δ_{Cd} fine structure contain nonadamantanoid species, also with $\{(\mu\text{-SPh})_3\text{CdSPh}\}$ and $\{(\mu\text{-SPh})_3\text{CdX}\}$ sites, such as the molecular species $[XCd_8(SPh)_{16}]^-$ with the structure already determined for $[ClZn_8(SPh)_{16}]^-$.[35] We find that DMF solutions of $Cd(SPh)_2$ containing $^1/_8X^-$ (X = Cl, Br, I) crystallize as structure **1a**, without halide incorporation, not as $[XCd_8(SPh)_{16}]^-$. Note that in $[XCd_8(SPh)_{16}]^-$ a single halide ion creates four $\{XCd(SPh)_3\}$ sites and thus could account for the high intensity of the halide-dependent resonance at $Q \leq 0.3$.

Addition of SPh^- to DMF solutions of **1a** also causes changes in the ^{113}Cd NMR. Upon addition of even small amounts of SPh^-, the minor line at 130 ppm disappears, consistent with the DMF in its coordination sphere being replaced by SPh^- ligands. With further addition of SPh^-, the NMR spectra are comprised of three major lines whose intensities vary with the solution composition ($Q = [SPh^-]/[Cd(SPh)_2]$). Up to $Q \approx 0.8$, the spectra are dominated by the line at 594 ppm. Subsequently, a line at 587 ppm becomes dominant, followed by a line at 606 ppm. By $Q = 4.0$, the only line observed is at 606 ppm.

Fuller details of the Cd NMR spectra of DMF solutions of $Cd(SPh)_2$ plus anionic ligands over the full range of Q and of temperature will be published separately. Nevertheless, the pronounced spectral changes with anion addition signify the electrophile character of at least some of the sites in the species present in DMF solutions of $Cd(SPh)_2$ and are further evidence against the occurrence of **4** in these solutions.

There is some comparable iron arenethiolate chemistry: $[Fe_3(SPh)_6(CO)_6]$ dissolved in THF with a small amount of DMSO crystallizes (after removal of CO) as $[Fe(DMSO)_6][Fe_4(SPh)_{10}]$.[36] We note also the existence of $[Cd_4(SPh)_8(PPh_3)_2]$.[37]

Summary

1. Crystalline compounds $_\infty[Cd(SAr)_2]$, which are structurally nonmolecular and comprised of vertex-linked adamantanoid cages, dissolve in DMF to form polycadmium macromolecules with extensive thiolate bridging.

2. These macromolecules appear to undergo rapid aggregation and deaggregation reactions, with an equilibrium distribution of large molecules at low temperature (ca. 225 K) and much smaller oligocadmium molecules at high temperature (ca. 340 K).

3. The ^{113}Cd and ^{13}C NMR spectra are consistent with vertex-linked adamantanoid cages as the structure type for the aggregates in solution. The postulated aggregate structures in solution are fragments of the known crystal structures.

4. The low ionic conductivity and the ^{113}Cd NMR data indicate that some ligand disproportionation occurs in solution, such that the larger oligoadamantanoid aggregates have small negative charges with SAr and DMF ligands distributed over peripheral terminal Cd coordination sites.

5. The aggregates in solution are electrophilic toward halide and thiolate ligands.

Experimental Section

Preparations and Crystallizations. The compounds were prepared as previously described, and purified by recrystallization from DMF by addition of ethanol.[4]

NMR. The ^{113}Cd spectra were measured at natural abundance in DMF, at 66.6 MHz with a Bruker CXP300 spectrometer, using 10-mm tubes in a multinuclear probe locked to acetone-d_6 in an insert. Proton decoupling was not used. Typical spectra required 3000–6000 pulses (20 μs; tip angle ca. 75°) with recycle delays of $\leq$2 s. Relaxation times T_1 were estimated by tests with variable recycle delay periods, in order to ensure that the relative intensities of resonances were not significantly distorted by saturation. All solutions were deoxygenated by sparging with N_2. Temperatures in the sample tube were controlled to ±1° and were calibrated by replacement with a sample tube containing a platinum thermometer. Chemical shifts are referenced to external 0.1 M aqueous $Cd(NO_3)_2$ as zero: this reference resonates at −5 ppm relative to aqueous $Cd(ClO_4)_2$ at infinite dilution.

^{13}C NMR spectra were measured on a JEOL FX-100 instrument at 25.05 MHz, with proton decoupling, and referenced to TMS. Small proportions of acetone were added to the DMF solutions for the lowest temperature measurements.

Conductivity. Conductivity measurements were obtained at 25 °C on solutions of $Cd(SPh)_2$, $(Me_4N)_2[Cd_4(SPh)_{10}]$, and Bu_4NI in DMF. Concentrations were varied through the range 0.1 to 5×10^{-5} M.

Molecular Weight. Because DMF is a very difficult solvent for molecular weight determinations by cryoscopic or osmometric methods (ebullioscopic data would not be relevant to the temperature range of the NMR data), cryoscopic measurements were made in HMPA. The low values of 290 ± 50 Da revealed that HMPA completely disrupted the aggregates and could not be regarded as comparable with DMF. Attempts to use the Signer isothermal distillation method in DMF are in progress.

Acknowledgment. Funding by the Australian Research Grants Scheme is gratefully acknowledged.

(35) Dance, I. G. *Aust. J. Chem.* **1985**, *38*, 1391.
(36) Walters, M. A.; Dewan, J. C. *Inorg. Chem.* **1986**, *25*, 4889.
(37) Black, S. J.; Einstein, F. W. B.; Hayes, P. C.; Kumar, R.; Tuck, D. G. *Inorg. Chem.* **1986**, *25*, 4181.

Contribution from the Department of Chemistry, York University, North York, Ontario, Canada M3J 1P3

Two-Electron Oxidation of Cobalt Phthalocyanines by Thionyl Chloride. Implications for Lithium/Thionyl Chloride Batteries

P. A. Bernstein and A. B. P. Lever*

Received July 14, 1989

Cyclic voltammetry, DPV, and electronic spectroscopy are used to study the reaction between thionyl chloride and cobalt phthalocyanine. $SOCl_2$ reacts with $[Co^ITnPc(2-)]^-$ and $Co^{II}TnPc(2-)$ to give two-electron-oxidized species. Implications for $Li/SOCl_2$ batteries are discussed. Thionyl chloride also forms a $SOCl_2$ monoadduct with $Co^{II}TnPc(2-)$. Driving forces (ΔE values) have been calculated for CoTnPc comproportionation and CoTnPc + $SOCl_2$ reactions. Rest potential measurements of a $Li/SOCl_2$ cell show that addition of $AlCl_3$ stabilizes the LiCl product as $LiAlCl_4$. A catalytic two-electron mechanism is indicated for the reduction of thionyl chloride in a $Li/SOCl_2/(CoTnPc,C)$ battery.

Introduction

The lithium/thionyl chloride ($SOCl_2$) cell is the highest energy density system known to date.[1] The battery consists of a lithium anode, a carbon cathode, an inorganic electrolyte, and thionyl chloride, which functions both as the solvent and cathode-active material. The most generally accepted cell reaction involves the formation of sulfur, sulfur dioxide, and lithium chloride.[2]

$$2SOCl_2 + 4Li \rightarrow S + SO_2 + 4LiCl$$

(1) Bowden, W. L.; Dey, A. N. *J. Electrochem. Soc.* **1980**, *127*, 1419.

0020-1669/90/1329-0608$02.50/0